Electrochemical Activation Parameters of Coupled Electron-Transfer and Spin-Exchange Reactions. Experimental Studies of $[M(Tacn)_2]^{3+/2+}$ and $[Fe(Pzb)_2]^{+/0}$ Redox Systems

Jeffrey W. Turner† and Franklin A. Schultz*

Department of Chemistry, Indiana University Purdue University Indianapolis, 402 North Blackford Street, Indianapolis, Indiana 46202-3274

Received: August 25, 2001; In Final Form: December 14, 2001

Expressions are derived for rate constants and activation parameters of electrochemical reactions that are accompanied by a change in spin-state. Predictions based on an electrochemical scheme of squares are compared with experimental results for $[M(tacn)_2]^{3+/2+}$ (M = Fe, Co, Ni, Ru; tacn = 1,4,7-triazacyclononane) and $[Fe(pzb)_2]^{+/0}$ (pzb^- = hydrotris(pyrazol-1-yl)borate $[HB(pz)_3^-]$, tetrakis(pyrazol-1-yl)borate $[B(pz)_4^-]$ or hydrotris(3,5-dimethylpyrazol-1-yl)borate $[HB(Me_2pz)_3^-]$) redox couples. The electrochemical rate constants, $(k_{s,h})_{obs}$, of $[Co(tacn)_2]^{3+/2+}$ and $[Fe\{HB(Me_2pz)_3\}_2]^{+/0}$ are decreased by the presence of spin-exchange. Electrochemical enthalpies ($\Delta H^{\ddagger}_{obs}$) and entropies ($\Delta S^{\ddagger}_{obs}$) of activation, determined from the temperature dependence of $(k_{s,h})_{obs}$ under nonisothermal cell conditions, provide evidence regarding the mechanism of these reactions. $[Co(tacn)_2]^{3+/2+}$, $[Fe(tacn)_2]^{3+/2+}$, and $[Fe\{HB(Me_2pz)_3\}_2]^{+/0}$ exhibit values of $\Delta H^{\ddagger}_{obs}$ and $\Delta S^{\ddagger}_{obs}$ that are larger than anticipated for simple electron-transfer, consistent with the interpretation that these reactions occur by coupled rather than concerted electron-transfer and spin-exchange and proceed through a high-spin intermediate in the M(III) oxidation state. Spin-exchange is viewed as a rapidly established, temperature-dependent equilibrium, the thermodynamic consequences of which are reflected in the electrochemical activation parameters.

Introduction

Electron-transfer reactions that are accompanied by a change in spin-state occur widely in chemistry and biology.[1] Such events can regulate biological function,[2] facilitate molecular device operation[3] and influence charge-transfer dynamics in condensed phases.[4] There is general agreement that presence of a spin-exchange decreases the rate of electron transfer. Prominent examples occur in cobalt-amine chemistry,[5] where chemical[6] and electrochemical[7] reductions of low-spin (LS) Co(III) to high-spin (HS) Co(II) complexes are slow. Although the subject has been discussed extensively,[8−14] the mechanism of these reactions (i.e., electron-transfer through a high-energy spin-state intermediate versus a concerted, three-electron event) and the basis of their kinetic inertness remain unclear.

The present study seeks to gain a clearer understanding of coupled electron-transfer and spin-exchange through measurement of electrochemical activation parameters. The influence of spin-state on electrochemical rate constants has been recognized for more than twenty years.[15−17] However, the thermal activation parameters of such reactions have received little attention. Perhaps this is so, because it is presumed that these quantities reflect only structural differences between reactants and products, as they do for simple electron transfer. However, we show that this is not the case when spin-exchange accompanies electron-transfer and that the electrochemical enthalpy and entropy of activation, $\Delta H^{\ddagger}_{obs}$ and $\Delta S^{\ddagger}_{obs}$,[18] which are obtained from the temperature dependence of the standard heterogeneous rate constant, $(k_{s,h})_{obs}$, measured under nonisothermal cell conditions,[19] provide unique mechanistic insight. The present article describes how $\Delta H^{\ddagger}_{obs}$ and $\Delta S^{\ddagger}_{obs}$ differ from values for simple electrode processes and how knowledge of these parameters can be used to characterize coupled electron-transfer and spin-exchange events.

The manuscript consists of three parts. The first part contains derivations of expressions for $(k_{s,h})_{obs}$, $\Delta H^{\ddagger}_{obs}$ and $\Delta S^{\ddagger}_{obs}$ for coupled electron-transfer and spin-exchange under nonisothermal cell conditions. The second part presents experimental results for two families of redox-active transition metal compounds: (1) a series of four $[M(tacn)_2]^{3+/2+}$ (M = Fe, Co, Ni, Ru; tacn = 1,4,7-triazacyclononane) complexes in which the presence of coupled electron-transfer and spin-exchange depends on the metal and (2) a series of three $[Fe(pzb)_2]^{+/0}$ (pzb^- = poly(pyrazol-1-yl)borate) couples in which the position of spin-equilibrium in the Fe(II) state is altered by changing ligand substituents. The third part discusses the significance of the observed activation parameters. We reported the parameters of the $[M(tacn)_2]^{3+/2+}$ half-reactions in an earlier publication[20] and noted that values of $\Delta H^{\ddagger}_{obs}$ and $\Delta S^{\ddagger}_{obs}$ for M = Fe and Co were unusually large. Results for the $[Fe(pzb)_2]^{+/0}$ couples are reported here for the first time. The structures of the ligands used in this study are illustrated in Chart 1.

Experimental Section

Materials. The compounds $[Fe\{B(pz)_4\}_2]$,[21] $[Fe\{HB(pz)_3\}_2]$,[21] $[Fe\{HB(Me_2pz)_3\}_2]$,[22] and $[Fe\{HB(Me_2pz)_3\}_2]PF_6$[23] were prepared by literature procedures from $FeCl_2 \cdot xH_2O$ (Alfa Aesar) and potassium salts of the ligands and characterized by cyclic voltammetry and ^1H NMR spectroscopy. Electrochemical solvents acetone and tetrahydrofuran (THF) (Burdick and Jackson) were obtained commercially and used as received. Tetra-*n*-butylammonium hexafluorophosphate ($TBAPF_6$) supporting electrolyte was purchased from SACHEM. Deuterated solvents were obtained from Aldrich.

Magnetic Susceptibility Measurements. Solution magnetic susceptibilities were determined in THF-d_8 by the ^1H NMR method of Evans[24] and employed a 200 MHz Varian Gemini spectrometer and TMS as the internal reference. Mass susceptibility was calculated from the expression $\chi_g = -3\Delta f/4\pi fm + \chi_o[1 + (d_o - d_s)/m]$,[25] where Δf is the frequency shift in Hz of the reference compound, f is the fixed probe frequency of the

* To whom correspondence should be addressed. Tel: (317) 278-2027. Fax: (317) 274-4701. E-mail: schultz@chem.iupui.edu.

† Present address: Bioanalytical Systems, Inc., 2701 Kent Avenue, West Lafayette, IN 47906.

10.1021/jp013294z CCC: $22.00
Published on Web 02/01/2002

CHART 1

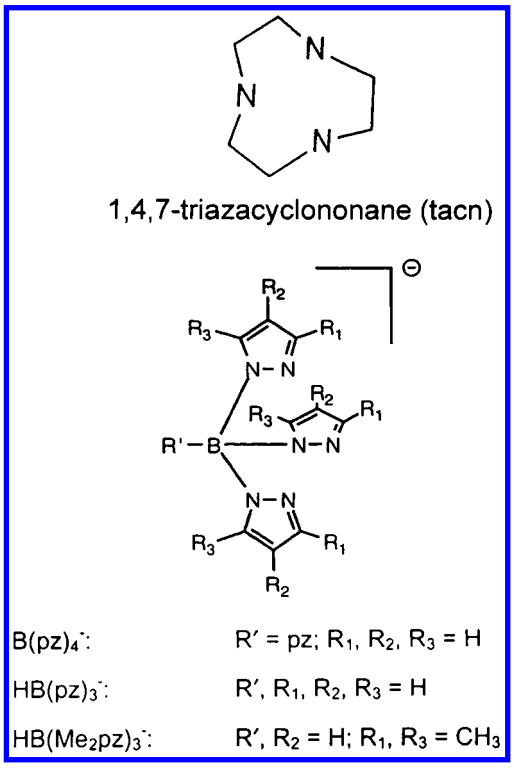

spectrometer, χ_o is the mass susceptibility of the solvent, m is the mass in grams of the complex in 1 cm^3 of solution, and d_o and d_s are the densities of the solvent and solution, respectively. The solution densities at 298 K were taken from the data of Binstead and Beattie,[26] and the temperature dependences of d_o and d_s were calculated from the data of Metz.[27] The molar susceptibility, $\chi_M = \chi_g \times$ MW, was corrected for the diamagnetic contributions of the ligands and Fe(II) core electrons to yield the corrected molar susceptibility, $\chi_{M'}$. The effective magnetic moment was calculated as $\mu_{eff} = 2.828(\chi_{M'}T)^{1/2}$. Thermodynamic parameters were obtained by fitting experimental values of μ_{eff} to eq 5 in ref 28.

Electrochemical Measurements. Conventional electrochemical measurements were made with a Bioanalytical Systems (BAS) 100A potentiostat. Fast scan cyclic voltammetry was performed using a laboratory-constructed three-electrode potentiostat following the design of Howell et al.[29] Its current-follower was a two-stage unit constructed on a separate circuit board and connected to the working electrode by a short lead to minimize stray capacitance. The potentiostat and electrochemical cell were housed in a Faraday cage. Cyclic voltammetric waveforms were generated by an EG&G PAR 175 universal programmer. Experimental traces were captured on a Nicolet 4094C digital oscilloscope, transferred to a personal computer and analyzed using a modified version of the Nicolet file transfer software (Henry, version 1.2). Electrode kinetic measurements were made in a nonisothermal three-electrode cell in which the reference electrode was maintained at ambient temperature and the working electrode temperature was varied from −40 to 20 °C by circulation of thermostated methanol using a low-temperature bath (FTS Model MC-4-80). Pt and Au microdisks with radii of 5 to 50 μm were used as working electrodes. The 12.5-, 25-, and 50-μm radius electrodes were constructed locally by published methods;[30] the 5-μm radius electrodes were purchased from BAS. Electrodes were polished with an aqueous suspension of 0.05-μm alumina (Buehler), sonicated in deionized water and rinsed with solvent before use. Diffusion coefficients, D, were measured by use of steady-state microelectrode voltammetry.[30] Identical values of D were assumed for oxidized and reduced forms. The resistivity, ρ, of electrolyte solutions was measured by use of a Yellow Springs Instrument conductivity bridge (Model 31) and dip-type cell (Model 3401).

SCHEME 1

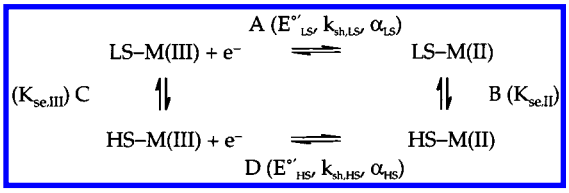

Heterogeneous electron-transfer rate constants, $(k_{s,h})_{obs}$, were determined from the sweep rate dependence of cyclic voltammetric peak potential separations, ΔE_p.[31] Electronic compensation of solution resistance was not employed. Rather, published guidelines[32] were used to select electrode sizes and sweep rate ranges that minimized contributions from uncompensated solution resistance, R_u, and nonlinear diffusion under a given set of experimental conditions. The existing R_u was accounted for by inclusion in digital simulations.[33] Voltammetric data were acquired as signal averages of 3 to 10 trials at seven scan rates (υ) covering a range of 2 orders of magnitude in υ at each temperature. Scan rate ranges of 100 to 10 000 V s^{-1} at 5- or 12.5-μm radius electrodes were employed for the $[Fe\{B(pz)_4\}_2]^{+/0}$ and $[Fe\{HB(pz)_3\}_2]^{+/0}$ couples and of 10 to 1000 V s^{-1} at 25- or 50-μm radius electrodes for the $[Fe\{HB(Me_2pz)_3\}_2]^{+/0}$ couple. These conditions produced peak potential separations of 80 to 200 mV, of which no more than 20 mV consisted of iR_u drop. Values of $(k_{s,h})_{obs}$ were obtained by fitting simulated voltammetric traces to experimental ones by use of Digisim (BAS, version 2.1).[34] Experimental values of reactant concentration, diffusion coefficient, electrode area, sweep rate, uncompensated solution resistance and double layer capacitance, C_{dl}, were used as input paramters for the simulations. R_u was determined as a function of temperature by use of the expression $R_u = \rho/4r$, where r is the electrode radius. The temperature dependence of ρ for 1:1 acetone/THF containing 0.3 M $TBAPF_6$ was defined by the relationship $\rho\ (\Omega\ cm) = 7.42\ e^{784/T}$ over the interval T = 233 to 293 K. The diffusion coefficients of $[Fe\{B(pz)_4\}_2]$, $[Fe\{HB(pz)_3\}_2]$ and $[Fe\{HB(Me_2pz)_3\}_2]$ were defined by D (cm^2 s^{-1}) = 0.000 685 $e^{-1276/T}$, 0.000 780 $e^{-1298/T}$ and 0.001 99 $e^{-1596/T}$, respectively, under the same conditions. C_{dl} (typically 15−25 μF cm^{-2}) was determined from the current in the non-Faradaic portion of each voltammogram. Simulations were conducted by allowing $k_{s,h}$ to vary until the simulated peak potential separation, $\Delta E_{p,sim}$, matched the experimental value, $\Delta E_{p,exp}$, to within 1 mV. If necessary, $\Delta E_{p,exp}$ was corrected for small (≤5 mV) contributions from nonlinear diffusion using the tabulation of Heinze.[35] Satisfactory fits were obtained with $\alpha = 0.50$. To test this approach $k_{s,h}$ and electrochemical activation parameters were determined for ferrocene oxidation in acetone containing 0.3 M $TBAPF_6$. The values obtained ($k_{s,h}$ = 2.0 ± 0.4 cm s^{-1}, $\Delta H^{\ddagger}$ = 16 ± 1 kJ mol^{-1} and $\Delta S^{\ddagger}$ = 1 ± 5 J mol^{-1} K^{-1}) are in good agreement with published results.[36]

Parameter Derivations

The electrochemical kinetics of coupled electron-transfer and spin-exchange are interpreted in terms of the "scheme of squares"[37−39] shown in Scheme 1. This mechanism is used widely to describe the influence of chemical reactions on accompanying charge-transfer events.[40−44] Steps A and D in Scheme 1 are electrode reactions that pertain to reduction and

reoxidation of the individual spin-state isomers. These reactions are assigned characteristic electrode potentials, $E^{\circ\prime}_i$, standard heterogeneous rate constants, $(k_{s,h})_i$, and transfer coefficients, α_i, where i = LS or HS. Steps B and C are the spin-exchange reactions in the individual oxidation states and are characterized by the spin-equilibrium constants, $K_{se,j}$, where j = II or III. Derivations for coupled electron-transfer and spin-exchange reactions are contrasted with those for electron-transfer directly across the square

$$\text{LS-M(III)} + e^- \rightleftharpoons \text{HS-M(II)} \quad (1)$$

Reaction 1 is assigned parameters ($E^{\circ\prime}$, $k_{s,h}$, α, $\Delta H^{\ddagger}$ and $\Delta S^{\ddagger}$) that correspond to a single, concerted event.

Rate Constants. Rate constants are defined in terms of classical Marcus−Hush theory for heterogeneous electron transfer[45−47]

$$k_{s,h} = Z_{el} \cdot \kappa_{el} \cdot \exp[-\Delta G^{\ddagger}_{el}/RT] \quad (2)$$

Z_{el} is the heterogeneous collisional frequency factor, κ_{el} is the electronic transmission coefficient and $\Delta G^{\ddagger}_{el}$ is the free energy of activation. Separation of $\Delta G^{\ddagger}_{el}$ into enthalpic and entropic components allows the rate constant to expressed as

$$k_{s,h} = Z_{el} \cdot \kappa_{el} \cdot \exp[\Delta S^{\ddagger}_{el}/R] \cdot \exp[-\Delta H^{\ddagger}_{el}/RT] \quad (3)$$

or

$$(k_{s,h})_{obs} = A \cdot \exp[\Delta S^{\ddagger}_{obs}/R] \cdot \exp[-\Delta H^{\ddagger}_{obs}/RT] \quad (4)$$

where $\Delta S^{\ddagger}_{obs} = \Delta S^{\ddagger}_{el} + R \ln(Z_{el} \cdot \kappa_{el}/A)$. For reactions occurring by a concerted mechanism, a small value of $k_{s,h}$ generally is considered to be the result of a large activation enthalpy arising from the significant inner- and outer-shell reorganizations that attend reduction of LS-M(III) to HS-M(II) and/or a small pre-exponential factor arising from a value of $\kappa_{el} < 1$ that corresponds to the "spin-forbidden" character of the reaction.The chemical change in reaction 1 also can be expressed in terms of a two-step mechanism consisting of coupled electron-transfer and spin-exchange as shown in Scheme 1. In this case, two routes are available for reduction of LS-M(III) to HS-M(II): a *low-spin pathway* (steps A plus B) consisting of electron transfer followed by spin-exchange and a *high-spin pathway* (steps C plus D) consisting of spin-exchange followed by electron transfer.[48] The "pure" electron-transfer rate constant within each coupled pathway should be larger than the $k_{s,h}$ for a concerted reaction, because inner-shell reorganization energies are small and $\kappa_{el} \approx 1$ for $(k_{s,h})_{LS}$ and $(k_{s,h})_{HS}$. However, $(k_{s,h})_{obs}$ will be diminished relative to $(k_{s,h})_{LS}$ or $(k_{s,h})_{HS}$, because the spin-equilibrium depletes the population of the electrochemically active form.

Expressions for the observed rate constants are obtained from a Butler−Volmer analysis[49] of coupled chemical and electrochemical reactions assuming that the chemical reactions (spin exchanges) remain in equilibrium.[50] Results for the low- and high-spin pathways are

$$(k_{s,h})_{obs,LS} = [1/(1 + K_{se,II})]^{\alpha,LS}\,[1/(1 + K_{se,III})]^{1-\alpha,LS}\,(k_{s,h})_{LS} = (x_{LS,II})^{\alpha,LS}\,(x_{LS,III})^{1-\alpha,LS}\,(k_{s,h})_{LS} \quad (5)$$

$$(k_{s,h})_{obs,HS} = [K_{se,II}/(1 + K_{se,II})]^{\alpha,HS}\,[K_{se,III}/(1 + K_{se,III})]^{1-\alpha,HS} \times (k_{s,h})_{HS} = (x_{HS,II})^{\alpha,HS}(x_{HS,III})^{1-\alpha,HS}(k_{s,h})_{HS} \quad (6)$$

where $x_{LS,j}$ and $x_{HS,j}$ are the spin-state mole fractions in the indicated oxidation state and $\Delta H^{\circ}_{se,j}$ and $\Delta S^{\circ}_{se,j}$ are the thermodynamic parameters of the indicated spin-equilibrium reaction

$$K_{se,j} = x_{HS,j}/x_{LS,j} = \exp[\Delta S^{\circ}_{se,j}/R] \cdot \exp[-\Delta H^{\circ}_{se,j}/RT] \quad (7)$$

The observed rate constant is the sum of terms for reaction through the two paths. Thus

$$(k_{s,h})_{obs} = (k_{s,h})_{obs,LS} + (k_{s,h})_{obs,HS} \quad (8)$$

It is useful to simplify the foregoing results for illustrative purposes. For example, it frequently is the case that spin-equilibrium is shifted extensively in one direction or the other in either or both oxidation states. A common occurrence is $x_{LS,III} \cong 1$ and/or $x_{HS,II} \cong 1$, in which case eqs 5 and 6 reduce to the following expressions, if it is assumed that $\alpha_{LS} = \alpha_{HS} = 0.5$[51]

$$(k_{s,h})_{obs,LS} \cong (x_{LS,II})^{1/2}\,(k_{s,h})_{LS} \quad (9)$$

$$(k_{s,h})_{obs,HS} \cong (x_{HS,III})^{1/2}\,(k_{s,h})_{HS} \quad (10)$$

When substituted into eq 8, eqs 9 and 10 demonstrate why slow electron-transfer kinetics frequently are observed for Co(III)/Co(II) couples, because both $x_{LS,II} \ll 1$ and $x_{HS,III} \ll 1$ for many of these systems.

Other workers have used the above or similar relationships to describe the influence of spin-state on electrochemical reactivity. Aoyagui derived expressions analogous to eqs 5, 6, and 8 and correlated them with rate constants for electrochemical reduction and oxidation of substituted tris(dithiocarbamato)iron-(III) complexes.[15] A qualitative correspondence was found, wherein electron-transfer reactions accompanied by a spin-state change were slower than those that were not. Kadish et al.[16,17] measured rate constants for reduction of substituted [Fe(III)-$(Salmeen)_2]^+$ and $[Fe(III)(Sal)_2trien]^+$ complexes[52] to high-spin Fe(II) products and found $(k_{s,h})_{obs}$ to increase with an increase in the mole fraction of high-spin Fe(III). The results of such studies establish that the rates of electrochemical reactions that involve a spin-state change are slower than those that do not and that $(k_{s,h})_{obs}$ varies with the distribution of spin-state forms. However, more detailed investigations have not been undertaken.

Activation Parameters. Electrochemical activation parameters provide an opportunity for more complete understanding of coupled electron-transfer and spin-exchange reactions. We consider the "real" enthalpies and entropies of activation[18,47] that are determined from the temperature dependence of $(k_{s,h})_{obs}$ measured under nonisothermal cell conditions.[19] The parameters are derived from eq 4 as

$$\Delta H^{\ddagger}_{obs} = -R\,\partial[\ln (k_{s,h})_{obs}]/\partial(1/T) \quad (11)$$

$$\Delta S^{\ddagger}_{obs} = R \ln (k_{s,h})_{obs} + \Delta H^{\ddagger}_{obs}/T - R \ln A \quad (12)$$

For the purpose of establishing $\Delta S^{\ddagger}_{obs}$ we assume $A = 2 \times 10^3$ cm s^{-1} based on a collisional frequency factor of $Z_{el} = (kT/2\pi M)^{1/2}$ for an $M = 300-600$ g $mole^{-1}$ reactant. Although this value is smaller than the 5×10^4 cm s^{-1} quantity predicted by the encounter preequilibrium model of electrochemical kinetics,[53] its use is consistent with previous practice in aqueous[20,54] and nonaqueous[55] media, wherein a factor of 2×10^3 cm s^{-1} affords a small value of $\Delta S^{\ddagger}_{obs}$—as anticipated for the intrinsic activation entropy of a simple adiabatic electrode reaction.[47] For coupled electron-transfer and spin-exchange occurring by

either of the mechanistic pathways in Scheme 1, the observed activation parameters are obtained from the inverse temperature derivative of the appropriate $\ln(k_{s,h})$ expression. For the low-spin pathway (eq 5)

$$(\Delta H^{\ddagger}_{obs})_{LS} = \Delta H^{\ddagger}_{LS} - \alpha_{LS}\, x_{HS,II}\, \Delta H^{\circ}_{se,II} - (1 - \alpha_{LS})\, x_{HS,III}\, \Delta H^{\circ}_{se,III} \quad (13)$$

$$(\Delta S^{\ddagger}_{obs})_{LS} = \Delta S^{\ddagger}_{LS} - \alpha_{LS}\, x_{HS,II}\, \Delta S^{\circ}_{se,II} - (1 - \alpha_{LS})\, x_{HS,III}\, \Delta S^{\circ}_{se,III} + \alpha_{LS}\, R \ln(x_{LS,II}) + (1 - \alpha_{LS})\, R \ln(x_{LS,III}) \quad (14)$$

where $\Delta H^{\ddagger}_{LS}$ and $\Delta S^{\ddagger}_{LS}$ are the activation parameters for reduction of LS-M(III) to LS-M(II). For the high-spin pathway (eq 6)

$$(\Delta H^{\ddagger}_{obs})_{HS} = \Delta H^{\ddagger}_{HS} + \alpha_{HS}\, x_{LS,II}\, \Delta H^{\circ}_{se,II} + (1 - \alpha_{HS})\, x_{LS,III}\, \Delta H^{\circ}_{se,III} \quad (15)$$

$$(\Delta S^{\ddagger}_{obs})_{HS} = \Delta S^{\ddagger}_{HS} + \alpha_{HS}\, x_{LS,II}\, \Delta S^{\circ}_{se,II} + (1 - \alpha_{HS})\, x_{LS,III}\, \Delta S^{\circ}_{se,III} + \alpha_{HS}\, R \ln(x_{HS,II}) + (1 - \alpha_{HS})\, R \ln(x_{HS,III}) \quad (16)$$

where $\Delta H^{\ddagger}_{HS}$ and $\Delta S^{\ddagger}_{HS}$ are the activation parameters for reduction of HS-M(III) to HS-M(II). At this stage of the analysis it is helpful to neglect the temperature dependence of the spin-state mole fractions and to assume that $x_{LS,II} = 0$, $x_{HS,III} = 0$, $\alpha_{HS} = 0.5$, and $\alpha_{LS} = 0.5$ and that terms in $R \ln(x_{i,j})$ are negligible. Under these conditions eqs 13−16 reduce to the following expressions

$$(\Delta H^{\ddagger}_{obs})_{LS} = \Delta H^{\ddagger}_{LS} - 0.5\,(x_{HS,II}\, \Delta H^{\circ}_{se,II}) \quad (17)$$

$$(\Delta S^{\ddagger}_{obs})_{LS} = \Delta S^{\ddagger}_{LS} - 0.5\,(x_{HS,II}\, \Delta S^{\circ}_{se,II}) \quad (18)$$

$$(\Delta H^{\ddagger}_{obs})_{HS} = \Delta H^{\ddagger}_{HS} + 0.5\,(x_{LS,III}\, \Delta H^{\circ}_{se,III}) \quad (19)$$

$$(\Delta S^{\ddagger}_{obs})_{HS} = \Delta S^{\ddagger}_{HS} + 0.5\,(x_{LS,III}\, \Delta S^{\circ}_{se,III}) \quad (20)$$

The results in eqs 13−20 illustrate the utility of electrochemical activation parameters in diagnosing the mechanism of coupled electron-transfer and spin-exchange. Spin-equilibria are entropically driven reactions, and $\Delta H^{\circ}_{se} > 0$ and $\Delta S^{\circ}_{se} > 0$ in all known instances. Therefore, $\Delta H^{\ddagger}_{obs}$ and $\Delta S^{\ddagger}_{obs}$ for electron transfer through the low-spin pathway will be *smaller* than values for comparable LS-M(III/II) half-reactions, whereas $\Delta H^{\ddagger}_{obs}$ and $\Delta S^{\ddagger}_{obs}$ for electron-transfer through the high-spin pathway will be *larger* than values for comparable HS-M(III/II) systems. It follows from eq 8 that the observed parameters will equal proportionate sums of eqs 17 and 19 and eqs 18 and 20, if the mechanism shares the two available pathways.

These conclusions are illustrated by the potential energy diagrams in Figure 1. In a nonisothermal electrochemical cell[19] the reference electrode is held at a fixed temperature, and $k_{s,h}$ is measured at the working electrode at the observed potential of the half-reaction in the absence of a thermodynamic driving force. Thus, the energies of the LS-M(III) reactant (LS^{3+}) and HS-M(II) product (HS^{2+}) are equal and remain so as temperature is varied. However, the temperature dependence of the spin-equilibrium reaction causes the relative positions of the LS and HS surfaces in each oxidation state to change with temperature. HS forms are favored by an increase in temperature. Therefore,

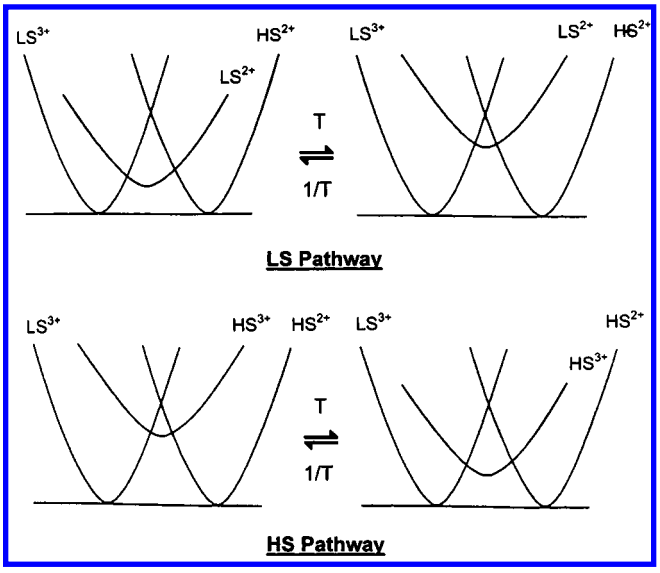

Figure 1. Potential energy curves for coupled electron-transfer and spin-exchange reactions.

if reaction proceeds through the low-spin intermediate, the low-spin M(II) state (LS^{2+}) is destabilized relative to HS^{2+} by an increase in temperature, and the apparent barrier height increases with increasing T (LS pathway). Conversely, if reaction proceeds through the high-spin M(III) state (HS^{3+}), this intermediate is stabilized relative to LS^{3+} by an increase in temperature, and the apparent barrier decreases with increasing T (HS pathway). Thus, when activation parameters are evaluated from the inverse temperature dependence of $\ln(k_{s,h})_{obs}$, the quantities $\Delta H^{\ddagger}_{obs}$ and $\Delta S^{\ddagger}_{obs}$ will be larger than anticipated in the event of the HS pathway and smaller than anticipated in the event of the LS pathway. These conclusions are consistent with the expressions derived in eqs 13 through 20.

In the event of concerted electron transfer, the enthalpy of activation will contain terms that reflect the entire inner- and outer-shell reorganizations that characterize reduction of LS-M(III) to HS-M(II). These quantities can be calculated from molecular properties and structural information. $\Delta H^{\ddagger}_{is}$ is obtained either from the harmonic oscillator model

$$\Delta H^{\ddagger}_{is} = N/2\, \Sigma\, f_i\, (\Delta a_i/2)^2 \quad (21)$$

where f_i is the reduced force constant for metal−ligand bond-stretching and Δa_i is the difference in metal−ligand bond distance between the two oxidation states, or from molecular mechanics calculations.[56] The outer-shell barrier is obtained from the mean sphere approximation[57]

$$\Delta H^{\ddagger}_{os} = Ne^2/8r[T(\partial\epsilon_{op}/\partial T)/\epsilon^2_{op} - (1 - 1/\epsilon_{op}) + \{(1 - 1/\epsilon_s) - T(\partial\epsilon_s/\partial T)/\epsilon^2_s\}/(1 + \delta_s/r) + T(1 - 1/\epsilon_s)(\partial\delta_s/\partial T)/r(1 + \delta_s/r)^2] \quad (22)$$

where ϵ_{op} and ϵ_s are the optical and static dielectric constants of the solvent, δ_s is the solvent polarization parameter, and r is the radius of the reactant. The rate of electron transfer also depends on the dynamical properties of solvent, which are represented by the inverse longitudinal relaxation time, τ_L^{-1}.[58] The temperature dependence of this parameter results in a longitudinal relaxation enthalpy, $\Delta H^{\ddagger}_{L}$, which contributes to the activation barrier.[57b,58b] Thus, the anticipated enthalpy of activation is calculated as the sum of the following terms[59−61]

$$\Delta H^{\ddagger}_{calc} = \Delta H^{\ddagger}_{is} + \Delta H^{\ddagger}_{os} + \Delta H^{\ddagger}_{L} \quad (23)$$

The entropy of activation consists of an outer-shell term that is obtained from the mean sphere approximation[57]

$$\Delta S^{\ddagger}_{os} = Ne^2/8r[(\partial\epsilon_{op}/\partial T)/\epsilon^2_{op} - (\partial\epsilon_s/\partial T)/\epsilon^2_s(1+\delta_s/r) +$$

$$(1 - 1/\epsilon_s)(\partial\delta_s/\partial T)/r(1 + \delta_s/r)^2] \quad (24)$$

plus a term in κ_{el} relating to the adiabaticity of the reaction. The anticipated entropy of activation is

$$\Delta S^{\ddagger}_{calc} = \Delta S^{\ddagger}_{os} + R \ln \kappa_{el} \quad (25)$$

The large inner-shell changes that characterize concerted electron transfer and spin-exchange result in a large value of $\Delta H^{\ddagger}_{is}$ which adds to the outer-shell barrier, $\Delta H^{\ddagger}_{os}$. However, $\Delta S^{\ddagger}_{os}$ is small (vide infra), and $\Delta S^{\ddagger}_{calc}$ can be less than zero, if $\kappa_{el} < 1$. Thus, eqs 21−25 predict that electron-transfer and spin-exchange reactions which occur by a concerted pathway will exhibit a large enthalpy of activation and a small or negative entropy of activation.

Results

The above derivations are considered in light of data from two experimental systems: a series of $[M(tacn)_2]^{3+/2+}$ half-reactions in which the position of spin-equilibrium in the M(II) state is varied by changing the metal (M = Fe, Co, Ni, Ru) and a series of $[Fe(pzb)_2]^{+/0}$ half-reactions in which the position of spin-equilibrium in the Fe(II) state is varied by changing substituents on the poly(pyrazolyl)borate ligand. Results for $[Fe(pzb)_2]^{+/0}$ couples are presented first.

$[Fe(pzb)_2]^{+/0}$ Half-Reactions. Iron-bis[poly(pyrazolyl)borate] complexes undergo the following electrode reaction in non-aqueous solvents

$$[Fe(III)(pzb)_2]^+ + e^- \rightleftharpoons [Fe(II)(pzb)_2] \quad (26)$$

Iron(III) complexes with $pzb^- = B(pz)_4^-$, $HB(pz)_3^-$ and $HB(Me_2pz)_3^-$ exhibit magnetic moments in dimethyl sulfoxide-d_6 solution at room temperature of 2.9, 2.5 and 2.7 μ_B, respectively. These values are consistent with low-spin Fe(III) in all cases, as found previously for $[Fe\{HB(Me_2pz)_3\}_2]^+$ in various solid forms.[23] The solution magnetic behavior of the iron(II) complexes in THF-d_8 is illustrated in Figure 2. $[Fe\{B(pz)_4\}_2]$ and $[Fe\{HB(Me_2pz)_3\}_2]$ exhibit temperature independent magnetic moments of 0.94 ± 0.09 and 4.78 ± 0.06 μ_B, respectively. These values establish $[Fe\{B(pz)_4\}_2]$ as low-spin and $[Fe\{HB(Me_2pz)_3\}_2]$ as high-spin under the experimental conditions. $[Fe\{HB(pz)_3\}_2]$ exhibits spin-equilibrium behavior, as indicated by its temperature-dependent magnetic moment. Values of $\Delta H^{\circ}_{se} = 24 \pm 1$ kJ mol^{-1}, $\Delta S^{\circ}_{se} = 70 \pm 2$ J mol^{-1} K^{-1} and $K_{se} = 0.078$ at 263 K are obtained from analysis of the data as described in the Experimental Section and compare favorably with an earlier determination by Beattie.[62,63] On the basis of these results reaction 26 is determined to be a LS-M(III) → LS-M(II) reduction in the case of $[Fe\{B(pz_4)\}_2]^{+/0}$, a LS-M(III) → HS-M(II) reduction in the case of $[Fe\{HB(Me_2pz)_3\}_2]^{+/0}$ and a LS-M(III) → LS/HS-M(II) reduction in the case of $[Fe\{HB(pz)_3\}_2]^{+/0}$.

Electrochemical rate data for the $[Fe(pzb)_2]^{+/0}$ couples were obtained in 1:1 acetone/THF containing 0.3 M $TBAPF_6$. This mixed solvent was chosen because $[Fe\{HB(Me_2pz)_3\}_2]$ is poorly soluble in polar, aprotic media, and it was desired to study all three half-reactions under identical solution conditions. Because of the choice of solvent and supporting electrolyte, uncompensated solution resistance (R_u) could not be avoided in the electrochemical measurements. The problem was addressed by adjusting electrode size, voltammetric scan rate and other experimental conditions to minimize iR_u drop[32] and by allowing for the presence of R_u in simulations of the experimental response.[33] A detailed description of procedures is given in the Experimental Section. Figure 3 shows an overlay of experimental and simulated current−potential curves for each $[Fe(pzb)_2]^{+/0}$ couple obtained under conditions that produce a kinetically meaningful separation of voltammetric peak potentials. It is evident that a much slower scan rate is needed to produce this result for $[Fe\{HB(Me_2pz)_3\}_2]^{+/0}$

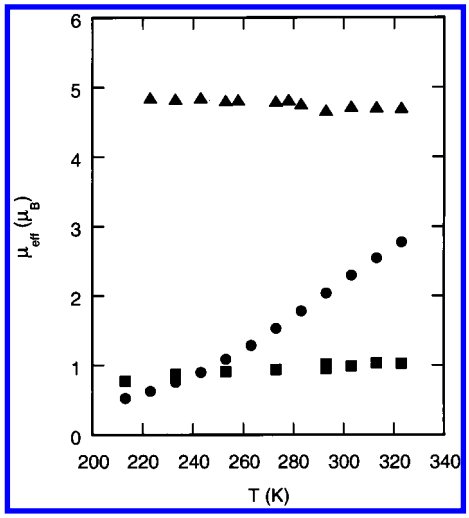

Figure 2. Effective magnetic moment as a function of temperature for $[Fe\{B(pz)_4\}_2]$ (■), $[Fe\{HB(Me_2pz)_3\}_2]$ (▲), and $[Fe\{HB(pz)_3\}_2]$ (●) in THF-d_8.

Table 1 contains electrochemical data and standard heterogeneous rate constants as a function of temperature for the $[Fe(pzb)_2]^{+/0}$ couples. Values of $(k_{s,h})_{obs}$ at 293 K for $[Fe\{B(pz_4)\}_2]^{+/0}$ and $[Fe\{HB(pz_3)\}_2]^{+/0}$ are large and close to the upper limit that can be determined accurately under the experimental conditions. The value of $(k_{s,h})_{obs}$ for $[Fe\{HB(Me_2pz)_3\}_2]^{+/0}$ at this temperature is more than 10 times smaller, consistent with the expectation that this electrode reaction is accompanied by a full change in spin-state. Electrochemical data have been reported for several $[Fe(pzb)_2]^{+/0}$ couples.[21,64,65] Zamponi et al.[64] measured electron-transfer rate constants in acetonitrile containing 0.3 M Et_4NClO_4 and reported values of $k_{s,h} = 0.013-0.015$ cm s^{-1} for the three couples considered here. These quantities are 1 to 2 orders of magnitude smaller than the rate constants in Table 1 and fail to exhibit a dependence on ligand substituent.

Plots of $\ln(k_{s,h})_{obs}$ versus $1/T$ determined over a temperature interval of 233−293 K for $[Fe\{B(pz_4)\}_2]^{+/0}$, $[Fe\{HB(pz_3)\}_2]^{+/0}$, and $[Fe\{HB(Me_2pz)_3\}_2]^{+/0}$ are shown in Figure 4. Values of $\Delta H^{\ddagger}_{obs}$ and $\Delta S^{\ddagger}_{obs}$ obtained from the slopes and intercepts are presented in Table 2. These parameters are compared with the quantities $\Delta H^{\ddagger}_{calc}$ and $\Delta S^{\ddagger}_{calc}$ calculated by use of eqs 23 and 25, respectively, for direct electron-transfer (i.e., an electrode reaction in which spin-exchange, if present, occurs in a concerted manner rather than as a preceding or following chemical step). The calculated parameters are obtained from $\Delta H^{\ddagger}_{is}$ values determined by molecular mechanics calculations,[56] $\Delta H^{\ddagger}_{os}$ and $\Delta S^{\ddagger}_{os}$ values calculated from eqs 22 and 24, respectively, using the structural information and solvent properties noted in Table 2, and $\Delta H^{\ddagger}_{L}$ values taken from the literature. It is assumed that

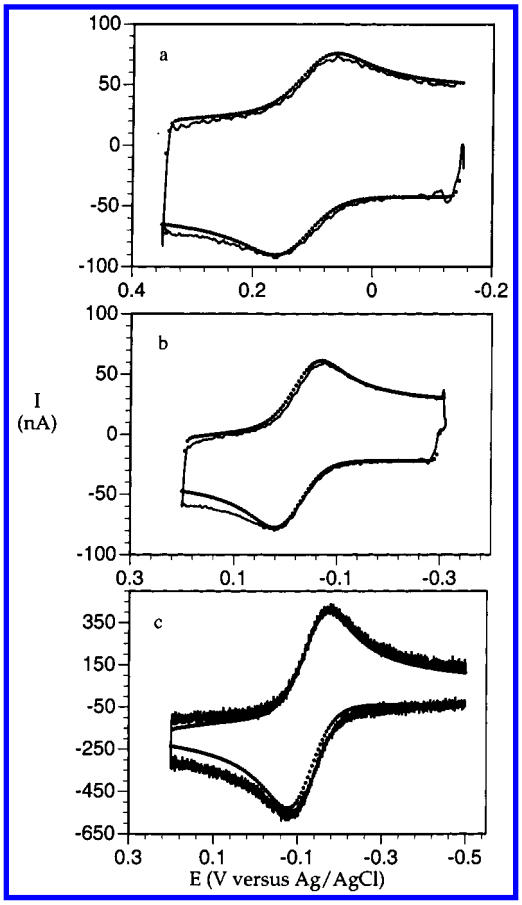

Figure 3. Overlay of experimental (—) and simulated (·····) current−potential curves for (a) $[Fe\{B(pz)_4\}_2]^{+/0}$ ($\upsilon = 2500$ V s^{-1}, $T = 253$ K, 5-μm radius, Au), (b) $[Fe\{HB(pz)_3\}_2]^{+/0}$ ($\upsilon = 2000$ V s^{-1}, $T = 253$ K, 5-μm radius, Au) and (c) $[Fe\{HB(Me_2pz)_3\}_2]^{+/0}$ ($\upsilon = 20$ V s^{-1}, $T = 293$ K, 50-μm radius, Pt) in 1:1 acetone/THF containing 0.3 M $TBAPF_6$.

TABLE 1: Electrochemical Data and Standard Heterogeneous Rate Constants as a Function of Temperature for $[Fe(pzb)_2]^{+/0}$ Couples[a]

	$[Fe\{B(pz)_4\}_2]^{+/0}$	$[Fe\{HB(pz)_3\}_2]^{+/0}$	$[Fe\{HB(Me_2pz)_3\}_2]^{+/0}$
	electrochemical data[b]		
$E^{\circ\prime}_{293}$ (V)	0.10 (1)	0.00 (1)	−0.12 (1)
ΔS°_{rc} (J mol^{-1} K^{-1})	78 (5)	76 (2)	96 (2)
T (K)		$(k_{s,h})_{obs}$ (cm s^{-1})	
293	1.5 (4)	2.2 (6)	0.09 (1)
283	0.75 (16)	2.0 (3)	0.067 (15)
273	0.62 (20)	1.4 (2)	0.044 (6)
263	0.43 (14)	1.2 (2)	0.027 (3)
253	0.28 (4)	0.9 (3)	0.019 (1)
243	0.25 (3)	0.72 (30)	0.008 (2)
233	0.14 (2)	0.44 (10)	0.004 (1)

[a] Measured for 1−3 mM solutions of complexes in 1:1 acetone/THF containing 0.3 M $TBAPF_6$ at Au ($[Fe\{B(pz)_4\}_2]^{+/0}$, $[Fe\{HB(pz)_3\}_2]^{+/0}$), or Pt ($[Fe\{HB(Me_2pz)_3\}_2]^{+/0}$) electrodes. [b] $E^{\circ\prime}_{293}$ is the observed potential in V versus Ag/AgCl of reaction 26 at 293 K. $\Delta S^{\circ}_{rc} = F(\partial E^{\circ\prime}/\partial T)$ is the electrode half-reaction entropy obtained over the interval 233−293 K.

$\kappa_{el} = 1$. $\Delta H^{\ddagger}_{os}$, $\Delta S^{\ddagger}_{os}$ and $\Delta H^{\ddagger}_{L}$ for 1:1 acetone/THF are assumed to equal the mean of the values calculated for the pure solvents. Although this simplification neglects possible selective solvation effects,[72] the physical properties of acetone and THF are similar.

$[Fe\{B(pz)_4\}_2]^{+/0}$ and $[Fe\{HB(pz)_3\}_2]^{+/0}$ exhibit values of $\Delta H^{\ddagger}_{obs} = 20$ and 15 kJ mol^{-1} and $\Delta S^{\ddagger}_{obs} = 8$ and −4 J mol^{-1} K^{-1}, respectively. These quantities are close to the activation parameters calculated for direct electron transfer without a spin-state change. The results are consistent with identification of the $[Fe\{B(pz)_4\}_2]^{+/0}$ couple as a LS-M(III) → LS-M(II) reduction and the $[Fe\{HB(pz)_3\}_2]^{+/0}$ couple as a LS-M(III) → LS/HS-M(II) reduction in which only 7% of the Fe(II) product is in the high-spin state at the 263 K midpoint of the temperature interval in Table 1. The $[Fe\{HB(Me_2pz)_3\}_2]^{+/0}$ half-reaction, which involves complete LS-M(III) → HS-M(II) conversion, exhibits values of $\Delta H^{\ddagger}_{obs} = 30$ kJ mol^{-1} and $\Delta S^{\ddagger}_{obs} = 19$ J mol^{-1} K^{-1} that exceed the quantities obtained for the other $[Fe(pzb)_2]^{+/0}$ couples as well as those calculated for direct electron transfer.

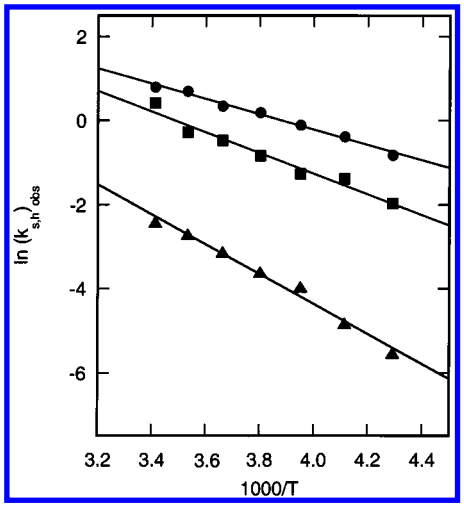

Figure 4. Plot of $\ln(k_{s,h})_{obs}$ versus $1/T$ for $[Fe\{B(pz)_4\}_2]^{+/0}$ (■), $[Fe\{HB(pz)_3\}_2]^{+/0}$ (●) and $[Fe\{HB(Me_2pz)_3\}_2]^{+/0}$ (▲) in 1:1 acetone/THF containing 0.3 M $TBAPF_6$.

$[M(tacn)_2]^{3+/2+}$ Half-Reactions. Electrochemical data for $[M(tacn)_2]^{3+/2+}$ half-reactions (eq 27), obtained in aqueous sodium fluoride solution and corrected for electrical double layer effects, are taken from ref 20

$$[M(tacn)_2]^{3+} + e^- \rightleftharpoons [M(tacn)_2]^{2+} \qquad (27)$$

These couples exhibit values of $(k_{s,h})_{obs}$ equal to 2.5, 1.3, 0.12, and 0.016 cm s^{-1} at 298 K for M = Fe, Ru, Ni, and Co, respectively, which correlate with the extent of M−N bond lengthening that accompanies reduction and with the square root of the corresponding homogeneous self-exchange rate constant, as predicted by Marcus−Hush theory.[45−47] However, a different pattern of behavior is reflected in the $\Delta H^{\ddagger}_{obs}$ and $\Delta S^{\ddagger}_{obs}$ values (Table 2).

$[Ru(tacn)_2]^{3+/2+}$ and $[Ni(tacn)_2]^{3+/2+}$ are adiabatic electrode reactions that do not involve a spin-state change and exhibit activation parameters characteristic of such a process. The $[Ru(tacn)_2]^{3+/2+}$ couple experiences little inner-shell reorganization and exhibits a value of $\Delta H^{\ddagger}_{obs} = 16$ kJ mol^{-1}, which is equal to the calculated outer-shell barrier height. A larger enthalpy of activation is determined for $[Ni(tacn)_2]^{3+/2+}$, which is attributed to the inner-shell structural change that accompanies addition of one antibonding electron to $[Ni(tacn)_2]^{3+}$. However, the experimental activation enthalpy (23 kJ mol^{-1}) is close to the sum of $\Delta H^{\ddagger}_{is}$ and $\Delta H^{\ddagger}_{os}$. For both $[Ru(tacn)_2]^{3+/2+}$ and $[Ni(tacn)_2]^{3+/2+}$ the magnitude of $\Delta S^{\ddagger}_{obs}$ is consistent with the expectation[47] that $\Delta S^{\ddagger}$ is close to zero for an adiabatic electrode reaction.

More complex behavior is exhibited by $[Fe(tacn)_2]^{3+/2+}$ and $[Co(tacn)_2]^{3+/2+}$. The isolated solids, $[Fe(tacn)_2]Cl_3 \cdot 5H_2O$ and

TABLE 2: Electrochemical Enthalpies (kJ mol^{-1}) and Entropies (J mol^{-1} K^{-1}) of Activation and Spin-state Characteristics for $[Fe(pzb)_2]^{+/0}$ [a] and $[M(tacn)_2]^{3+/2+}$ [b] Couples

redox couple	$\Delta H^{\ddagger}_{is}$ [c]	$\Delta H^{\ddagger}_{os}$ [d]	$\Delta H^{\ddagger}_{L}$ [e]	$\Delta H^{\ddagger}_{calc}$ [f]	$\Delta H^{\ddagger}_{obs}$	$\Delta S^{\ddagger}_{os}$ [d]	$\Delta S^{\ddagger}_{calc}$ [g]	$\Delta S^{\ddagger}_{obs}$	spin-state change
$[Fe\{B(pz)_4\}_2]^{+/0}$	1	11	5	17	20(2)	2	2	8(7)	
$[Fe\{HB(pz)_3\}_2]^{+/0}$	1	11	5	17	15(1)	2	2	−4(3)	LS-M(III) → LS/HS-M(II)
$[Fe\{HB(Me_2pz)_3\}_2]^{+/0}$	1	11	5	17	30(2)	2	2	19(6)	LS-M(III) → HS-M(II)
$[Ru(tacn)_2]^{3+/2+}$	0	16	0	16	16(2)	1	1	−7(8)	
$[Ni(tacn)_2]^{3+/2+}$	6	16	0	22	23(2)	1	1	−4(8)	
$[Fe(tacn)_2]^{3+/2+}$	1	16	0	17	27(1)	1	1	35(4)	LS-M(III) → LS/HS-M(II)
$[Co(tacn)_2]^{3+/2+}$	25	16	0	41	70(3)	1	1	137(10)	LS-M(III) → HS-M(II)

[a] Electrochemical data obtained in 1:1 acetone/THF containing 0.3 M $TBAPF_6$ at Au ($[Fe\{B(pz)_4\}_2]^{+/0}$, $[Fe\{HB(pz)_3\}_2]^{+/0}$), or Pt ($[Fe\{HB(Me_2pz)_3\}_2]^{+/0}$) electrodes. [b] Electrochemical data obtained in aqueous 0.75 M NaF and corrected for temperature-dependent electrical double layer effects at Pt (Ru, Ni) or Hg (Fe, Co) electrodes (ref 20). [c] From molecular mechanics calculations (ref 56); values for $[Fe(pzb)_2]^{+/0}$ couples assumed equal to that calculated for LS-$[Fe(tacn)_2]^{3+}$ to LS-$[Fe(tacn)_2]^{2+}$ reduction. [d] From eqs 22 and 24 by use of $\epsilon_{op} = 1.839$, $\partial\epsilon_{op}/\partial T = -0.001\,36$, $\epsilon_s = 20.7$, $\partial\epsilon_s/\partial T = -0.0977$, $\delta_s = 80$ pm, and $\partial\delta_s/\partial T = 0.07$ pm K^{-1} for acetone; $\epsilon_{op} = 1.974$, $\partial\epsilon_{op}/\partial T = -0.001\,24$, $\epsilon_s = 7.58$, $\partial\epsilon_s/\partial T = -0.030$, $\delta_s = 80$ pm, and $\partial\delta_s/\partial T = 0.07$ pm K^{-1} for THF; $\epsilon_{op} = 1.776$, $\partial\epsilon_{op}/\partial T = -0.000\,25$, $\epsilon_s = 78.39$, $\partial\epsilon_s/\partial T = -0.360$, $\delta_s = 82.6$ pm, and $\partial\delta_s/\partial T = 0.036$ pm K^{-1} for H_2O; $r = 510$ pm for $[Fe(pzb)_2]^{+/0}$ couples (ref 66); $r = 430$ pm for $[M(tacn)_2]^{3+/2+}$ couples (ref 20); ϵ_{op}, ϵ_s and $\partial\epsilon_s/\partial T$ from ref 67; $\partial\epsilon_{op}/\partial T$ from ref 68; δ_s and $\partial\delta_s/\partial T$ from refs 57b and 69 (values for THF assumed equal to those of acetone). $\Delta H^{\ddagger}_{os}$ and $\Delta S^{\ddagger}_{os}$ for 1:1 acetone/THF equal mean of values calculated for the pure solvents. [e] Mean value of $\Delta H^{\ddagger}_{L} = 3.6$ kJ mol^{-1} for acetone (ref 57a) and $\Delta H^{\ddagger}_{L} = 7$ kJ mol^{-1} for THF (ref 70); $\Delta H^{\ddagger}_{L} = 0$ assumed for H_2O.[71] [f] Equation 23. [g] Equation 25.

$[Fe(tacn)_2]Cl_2 \cdot 4H_2O$, have been characterized as low-spin complexes[73] and there is little difference between the Fe(III)-N and Fe(II)-N bond distances of these compounds. Thus, a large activation barrier is not anticipated for $[Fe(tacn)_2]^{3+}$ to $[Fe(tacn)_2]^{2+}$ reduction. However, we recently demonstrated that $[Fe(tacn)_2]^{2+}$ undergoes $^1A_{1g} \rightarrow {}^5T_{2g}$ spin-exchange in solution and determined values of $\Delta H^{\circ}_{se} = 24$ kJ mol^{-1}, $\Delta S^{\circ}_{se} = 68$ J mol^{-1} K^{-1} and $K_{se} = 0.19$ at 293 K in D_2O for this equilibrium.[28,74] Detection of this reaction and recognition that electron-transfer proceeds with partial LS-M(III) → HS-M(II) spin conversion provides an explanation for the observation that $\Delta H^{\ddagger}_{obs} = 27$ kJ mol^{-1} and $\Delta S^{\ddagger}_{obs} = 35$ J mol^{-1} K^{-1} for $[Fe(tacn)_2]^{3+/2+}$.

The $[Co(tacn)_2]^{3+/2+}$ half-reaction is characterized by complete LS-M(III) → HS-M(II) spin exchange. There is an 18.1 pm difference between the Co(III)-N bond distance in [Co((R)-Metacn)$_2$]$I_3 \cdot 5H_2O$[75] and the Co(II)-N bond distance in [Co(tacn)$_2$]$I_2 \cdot 2H_2O$.[76] From this structural information we calculated an inner-shell barrier height of 25 kJ mol^{-1} by molecular mechanics.[56] Addition of an outer-shell barrier of 16 kJ mol^{-1} yields $\Delta H^{\ddagger}_{calc} = 41$ kJ mol^{-1}. However, the experimental barrier height of $\Delta H^{\ddagger}_{obs} = 70$ kJ mol^{-1} is much larger than this quantity. In addition, $[Co(tacn)_2]^{3+/2+}$ exhibits an entropy of activation ($\Delta S^{\ddagger}_{obs}$) of 137 J mol^{-1} K^{-1}. Thus, the observed activation parameters of $[Co(tacn)_2]^{3+/2+}$ are inconsistent with concerted electron-transfer and spin-exchange.

Discussion

This investigation compares rate constants and activation parameters of electrode reactions that are accompanied by a change in spin-state with those that are not. One objective is to obtain evidence regarding the mechanism of parallel electron-transfer and spin-exchange reactions. Activation parameters measured under nonisothermal cell conditions provide insight to this question.

The $[Co(tacn)_2]^{3+/2+}$ and $[Fe\{HB(Me_2pz)_3\}_2]^{+/0}$ half-reactions undergo reduction with complete LS-M(III) → HS-M(II) conversion. These couples exhibit comparatively small values of $(k_{s,h})_{obs}$ as predicted by eqs 8−10. However, observation of enhanced $\Delta H^{\ddagger}_{obs}$ and $\Delta S^{\ddagger}_{obs}$ values relative to $\Delta H^{\ddagger}_{calc}$ and $\Delta S^{\ddagger}_{calc}$ provides evidence that these reactions proceed by a coupled mechanism (Scheme 1) rather than a concerted one. The magnitude of $\Delta S^{\ddagger}_{obs}$, which reflects the adiabaticity of the reaction, is an important consideration in the matter. Various estimates have placed κ_{el} in the range of 10^{-4} to 10^{-2} for the homogeneous self-exchange of $[Co(NH_3)_6]^{3+/2+}$,[9,13] although it is likely that κ_{el} is larger for diffusing reactants at an electrode surface.[77] However, as κ_{el} cannot exceed unity, electrochemical reactions that proceed by a concerted mechanism should exhibit $\Delta S^{\ddagger}_{obs} \leq 0$. Observation that $\Delta S^{\ddagger}_{obs} \gg 0$ in conjunction with unusually large $\Delta H^{\ddagger}_{obs}$ values for $[Co(tacn)_2]^{3+/2+}$ and $[Fe\{HB(Me_2pz)_3\}_2]^{+/0}$ supports a mechanism of coupled electron-transfer and spin-exchange for these half-reactions. The $[Fe(tacn)_2]^{3+/2+}$ couple, which proceeds with partial LS-M(III) → HS-M(II) conversion, but does not display a small $(k_{s,h})_{obs}$ value, also exhibits activation parameters that indicate involvement of a spin-equilibrium step. The $[Ru(tacn)_2]^{3+/2+}$, $[Ni(tacn)_2]^{3+/2+}$, and $[Fe\{B(pz)_4\}_2]^{+/0}$ couples, which undergo electron transfer without a spin exchange, have rate constants and activation parameters that are characteristic of a simple adiabatic reaction, and the $[Fe\{HB(pz)_3\}_2]^{+/0}$ couple, which is characterized by a small proportion of LS-M(III) → HS-M(II) conversion, exhibits $\Delta H^{\ddagger}_{obs}$ and $\Delta S^{\ddagger}_{obs}$ values that are not greatly from those of such a process.

Two aspects of the data in Table 2 are of particular interest. One is the fact that the three half-reactions which display clear evidence of coupled electron-transfer and spin-exchange—$[Co(tacn)_2]^{3+/2+}$, $[Fe(tacn)_2]^{3+/2+}$ and $[Fe\{HB(Me_2pz)_3\}_2]^{+/0}$—have activation parameters that indicate a preference for the HS pathway (eq 17−20). This is so even for $[Fe(tacn)_2]^{3+/2+}$, wherein the low-spin form of $[Fe(tacn)_2]^{2+}$ predominates under the experimental conditions.[78] Moreover, the indicated preference for a HS pathway in the electrochemical reduction of $[Co(tacn)_2]^{3+}$ is unanticipated, because previous interpretations that have favored a coupled mechanism for $[CoN_6]^{3+/2+}$ self-exchange have identified the low-spin form of Co(II) as the likely intermediate.[8,11,12,14] This conclusion is based on estimates[11−13] that the ^2E_g excited state of $[Co(NH_3)_6]^{2+}$ lies only 3000−9000 cm^{-1} above the $^4T_{1g}$ ground state. The probable high-spin Co(III) intermediate is the $^3T_{1g}$ state,[13] which for $[Co(NH_3)_6]^{3+}$ lies 13 000−13 700 cm^{-1} above the $^1T_{1g}$ ground state.[79] Although spectroscopic data from which excited-state energies of $[Co(tacn)_2]^{3+}$ and $[Co(tacn)_2]^{2+}$ can be estimated are unavailable, a larger energy gap in the Co(III) versus Co(II) oxidation state does not preclude reaction via the HS pathway. We believe this is so, because energy differences between spectroscopic ground and excited states are enthalpic in nature and do not reflect the large entropic contributions that characterize thermally equilibrated spin-exchange reactions.[74,80] These entropic terms, which arise from differences in vibrational

and electronic properties,[74,81] strongly favor HS over LS forms with increasing temperature. Thus, thermally equilibrated electron-transfer reactions may proceed via a HS-M(III) form, although this spin-state may appear from spectroscopic measurements to be the higher energy intermediate.

A second aspect of the data in Table 2 is the extent to which the activation parameters of $[Fe(pzb)_2]^{+/0}$ half-reactions are influenced relative to those of $[M(tacn)_2]^{3+/2+}$ by the presence of a spin-equilibrium. Thus, the amounts by which $\Delta H^{\ddagger}_{obs}$ and $\Delta S^{\ddagger}_{obs}$ exceed $\Delta H^{\ddagger}_{calc}$ and $\Delta S^{\ddagger}_{calc}$ are much smaller for $[Fe\{HB(Me_2pz)_3\}_2]^{+/0}$ than they are for $[Co(tacn)_2]^{3+/2+}$, although both half-reactions involve full LS-M(III) → HS-M(II) conversion. In addition, smaller activation parameter differences are observed for $[Fe\{HB(pz)_3\}_2]^{+/0}$ in comparison with $[Fe(tacn)_2]^{3+/2+}$, although both couples are characterized by a partial LS-M(III) → LS/HS-M(II) spin-exchange. One explanation of this behavior is that thermodynamic spin-equilibrium parameters are larger for tacn complexes than they are for pzb^- species. The parameters needed to explore this possibility have not been measured. A second explanation is that poly(pyrazolyl)-borate complexes may exhibit a greater preference for the LS pathway than their tacn counterparts. The fact that small values of $\Delta H^{\ddagger}_{obs}$ and $\Delta S^{\ddagger}_{obs}$ are observed for $[Fe\{HB(pz)_3\}_2]^{+/0}$ relative to the LS-M(III) → LS-M(II) reduction of $[Fe\{B(pz)_4\}_2]^{+/0}$ may reflect this tendency. However, the differences in $\Delta H^{\ddagger}_{obs}$ and $\Delta S^{\ddagger}_{obs}$ are small relative to the experimental uncertainty, which makes evaluation of this possibility difficult.

Conclusions

Rate constants and activation parameters of electrochemical reactions that are accompanied by a change in spin-state differ from those of simple electron transfer. Magnitudes of $\Delta H^{\ddagger}_{obs}$ and $\Delta S^{\ddagger}_{obs}$ obtained under nonisothermal cell conditions provide evidence regarding the mechanism of electron-transfer and spin-exchange. Experimental studies indicate that the $[Co(tacn)_2]^{3+/2+}$, $[Fe(tacn)_2]^{3+/2+}$, and $[Fe\{HB(Me_2pz)_3\}_2]^{+/0}$ half-reactions undergo electron-transfer and spin-exchange by a coupled rather than a concerted mechanism and that the probable pathway favors electron transfer through a high-spin intermediate in the M(III) oxidation state. Spin-exchange is viewed as a rapidly established chemical equilibrium that influences charge transfer dynamics through the thermodynamic driving force imparted as a pre- or post- charge-transfer event. Its important consequences are to decrease the rate of electron-transfer by depleting the population of electrochemically active forms and to make thermodynamic contributions to the electrochemical enthalpy and entropy of activation.

Acknowledgment. This work is supported by a grant from the National Science Foundation (CHE-9988694). J.W.T. acknowledges support from an Eli Lilly Graduate Summer Fellowship.

References and Notes

(1) Turner, J. W.; Schultz, F. A. *Coord. Chem. Rev.* **2001**, *219*−*221*, 81.
(2) Mueller, E. J.; Lioda, P. J.; Sligar, S. G. In *Cytochrome P450: Structure, Mechanism and Biochemistry*, 2nd ed.; Ortiz de Montellano, P. R., Ed.; Plenum Press: New York, 1995, Chapter 3.
(3) Balzani, V.; Credi, A.; Raymo, F. M.; Stoddart, J. F. *Angew. Chem., Int. Ed. Engl.* **2000**, *39*, 3348.
(4) Williams, M. E.; Masui, H.; Long, J. W.; Malik, J.; Murray, R. W. *J. Am. Chem. Soc.* **1997**, *119*, 1997.
(5) Hendry, P.; Ludi, A. *Adv. Inorg. Chem.* **1990**, *35*, 117.
(6) Meyer, T. J.; Taube, H. In *Comprehensive Coordination Chemistry*, Wilkinson, G., Gillard, R. D., McCleverty, J. A., Eds.; Pergamon Press: Oxford, 1987; Volume 1, Chapter 7.2.
(7) Weaver, M. J. *J. Electroanal. Chem.* **2001**, *498*, 105.
(8) Stynes, H. C.; Ibers, J. A. *Inorg. Chem.* **1971**, *10*, 2304.
(9) Buhks, E.; Bixon, M.; Jortner, J.; Navon, G. *Inorg. Chem.* **1979**, *18*, 2014.
(10) Siders, P.; Marcus, R. A. *J. Am. Chem. Soc.* **1981**, *103*, 741.
(11) Larsson, S.; Ståhl, K.; Zerner, M. C. *Inorg. Chem.* **1986**, *25*, 3033.
(12) Geselowitz, D. *Inorg. Chim. Acta* **1989**, *163*, 79.
(13) Newton, M. D. *J. Phys. Chem.* **1991**, *95*, 30.
(14) Shalders, R. D.; Swaddle, T. W. *Inorg. Chem.* **1995**, 34, 4815.
(15) Yasuda, H.; Suga, K.; Aoyagui, S. *J. Electroanal. Chem.* **1978**, *86*, 259.
(16) Kadish, K. M.; Su, C. H.; Wilson, L. J. *Inorg. Chem.* **1982**, *21*, 2312.
(17) Zhu, T.; Su, C.-H.; Schaeper, D.; Lemke, B. K.; Wilson, L. J.; Kadish, K. M. *Inorg. Chem.* **1984**, *23*, 4345.
(18) Weaver, M. J. *J. Phys. Chem.* **1979**, *83*, 1748.
(19) Yee, E. L.; Cave, R. J.; Guyer, K. L.; Tyma, P.; Weaver, M. J. *J. Am. Chem. Soc.* **1979**, *101*, 1131.
(20) Crawford, P. W.; Schultz, F. A. *Inorg. Chem.* **1994**, *33*, 4344.
(21) Trofimenko, S. *J. Am. Chem. Soc.* **1967**, *89*, 3170.
(22) Trofimenko, S. *J. Am. Chem. Soc.* **1967**, *89*, 6288.
(23) Mason, S. J.; Hill, C. M.; Murphy, V. J.; O'Hare, D.; Watkin, D. J. *J. Organomet. Chem.* **1995**, *485*, 165.
(24) Evans, D. F. *J. Chem. Soc.* **1959**, 2003.
(25) Naklicki, M. L.; White, C. A.; Plante, L. L.; Evans, C. E. B.; Crutchley, R. J. *Inorg. Chem.* **1998**, *37*, 1880.
(26) Binstead, R. A.; Beattie, J. K. *Inorg. Chem.* **1986**, *25*, 1481.
(27) Metz, D. J.; Glines, A. *J. Phys. Chem.* **1967**, *71*, 1158.
(28) Turner, J. W.; Schultz, F. A. *Inorg. Chem.* **2001**, *40*, 5296.
(29) Howell, J. O.; Kuhr, W. G.; Ensman, R. E.; Wightman, R. M. *J. Electroanal. Chem.* **1986**, *209*, 77.
(30) Wightman, R. M.; Wipf, D. O. *Electroanal. Chem.* **1989**, *15*, 267.
(31) Nicholson, R. S. *Anal. Chem.* **1965**, *37*, 1351.
(32) Bowyer, W. J.; Engelman, E. E.; Evans, D. H. *J. Electroanal. Chem.* **1989**, *262*, 67.
(33) Safford, L. K.; Weaver, M. J. *J. Electroanal Chem.* **1991**, *312*, 69.
(34) Rudolph, M.; Reddy, D. R.; Feldberg, S. W. *Anal. Chem.* **1994**, *66*, 589A.
(35) Heinze, J. *Ber. Bunsen-Ges. Phys. Chem.* **1981**, *85*, 1096.
(36) Safford, L. K.; Weaver, M. J. *J. Electroanal Chem.* **1992**, *331*, 857.
(37) Jacq, J. *J. Electroanal. Chem.* **1971**, *29*, 149.
(38) Bond, A. M.; Oldham, K. B. *J. Phys. Chem.* **1983**, *87*, 2492.
(39) Lerke, S. A.; Evans, D. H.; Feldberg, S. W. *J. Electroanal. Chem.* **1990**, *296*, 299.
(40) Laviron, E.; Roullier, L. *J. Electroanal. Chem.* **1985**, *186*, 1.
(41) Evans, D. H.; O'Connell, K. M. *Electroanal. Chem.* **1986**, *14*, 113.
(42) Martin, M. J.; Endicott, J. F.; Ochrymowycz, L. A.; Rorabacher, D. B. *Inorg. Chem.* **1987**, *26*, 3012.
(43) Brunschwig, B. S.; Sutin, N. *J. Am. Chem. Soc.* **1989**, *111*, 7454.
(44) Gray, H. B.; Winkler, J. R. *Annu. Rev. Biochem.* **1996**, *65*, 537.
(45) Marcus, R. A. *J. Chem. Phys.* **1965**, *43*, 679.
(46) Hush, N. S. *Trans. Faraday Soc.* **1961**, *57*, 557.
(47) Weaver, M. J. In *Comprehensive Chemical Kinetics*; Compton, R. G., Ed.; Elsevier: Amsterdam, 1987; Volume 27, pp 1−60.
(48) Derivations are presented for a LS-M(III) → HS-M(II) conversion, because this circumstance corresponds to the more frequent observation (based on ligand field strength considerations) that low-spin behavior is favored in the higher oxidation state and high-spin behavior is favored in the lower oxidation state.
(49) Bard, A. J.; Faulkner, L. R. *Electrochemical Methods: Fundamentals and Applications*, 2nd ed.; Wiley: New York, 2001.
(50) This assumption is based on the observation that rate constants of spin-exchange reactions are on the order of 10^6 to 10^9 s^{-1}: Beattie, J. K. *Adv. Inorg. Chem.* **1988**, *32*, 1.
(51) This assumption is based on the expectation that inner-shell reorganization energies will be small and energy barriers will be symmetric for electrode reactions involving a single spin-state. The transfer coefficient will be close to 0.5 under these circumstances.
(52) $Salmeen^-$ is the tridentate Schiff base ligand prepared by condensation of salicylaldehyde and *N*-methylethylenediamine; $(Sal)_2trien^{2-}$ is the hexadentate Schiff base ligand prepared by condensation of salicylaldehyde and triethylenetetramine.
(53) Hupp, J. T.; Weaver, M. J. *J. Electroanal. Chem.* **1983**, *152*, 1.
(54) Farmer, J. K.; Gennett, T.; Weaver, M. J. *J. Electroanal. Chem.* **1985**, *191*, 357.
(55) (a) Anxolabéhère, E.; Lexa, D.; Savéant, J.-M. *J. Phys. Chem.* **1992**, *96*, 1266. (b) Antonello, A.; Formaggio, F.; Moretto, A.; Toniolo, C.; Maran, F. *J. Am. Chem. Soc.* **2001**, *123*, 9577.
(56) Gao, Y.-D.; Lipkowitz, K. B.; Schultz, F. A. *J. Am. Chem. Soc.* **1995**, *117*, 11932.
(57) (a) Fawcett, W. R.; Blum, L. *Chem. Phys. Lett.* **1991**, *187*, 173. (b) Fawcett, W. R.; Opallo, M. *J. Phys. Chem.* **1992**, *96*, 2920.

(58) (a) Weaver, M. J. *Chem. Rev.* **1992**, *92*, 463. (b) Fawcett, W. R.; Opallo, M. *Angew. Chem., Int. Ed. Engl.* **1994**, *33*, 2131.

(59) Although a fractional contribution from $\Delta H^{\ddagger}_{L}$ is anticipated in some circumstances,[60] a linear dependence of $k_{s,h}$ on τ_L^{-1} often is observed.[61] Thus, the full value of $\Delta H^{\ddagger}_{L}$ is included in eq 23.

(60) Sumi, H.; Marcus, R. A. *J. Chem. Phys.* **1986**, *84*, 4894.

(61) (a) Nielson, R. M.; Weaver, M. J. *J. Electroanal. Chem.* **1989**, *15*, 260. (b) Mu, X. H.; Schultz, F. A. *J. Electroanal. Chem.* **1993**, *353*, 349. (c) Winkler, K.; Baranski, A. S.; Fawcett, W. R. *J. Chem. Soc., Faraday Trans.* **1996**, *92*, 3899.

(62) Beattie, J. K.; Binstead, R. A.; West, R. J. *J. Am. Chem. Soc.* **1978**, *100*, 3044.

(63) Although the electrochemical and magnetic susceptibility measurements are conducted in different solvents, it is anticipated that the influence of solvent on the thermodynamic parameters of the spin-crossover reaction will be small as indicated by our recent demonstration of the solvent independence of the $[Fe(tacn)_2]^{2+}$ spin-equilibrium.[28]

(64) Zamponi, S.; Gambini, G.; Conti, P.; Gioia Lobbia, G.; Marassi, R.; Berrettoni, M.; Cecchi, P. *Polyhedron* **1995**, *14*, 1929.

(65) Janiak, C.; Scharmann, T. G.; Green, J. C.; Parkin, R. P. G.; Kolm, M. J.; Riedel, E.; Mickler, W.; Elguero, J.; Claramunt, R. M.; Sanz, D. *Chem.−Eur. J.* **1996**, *2*, 992.

(66) Sohrin, Y.; Kokusen, H.; Matsui, M. *Inorg. Chem.* **1995**, *34*, 3928.

(67) Marcus, Y. *Ion Solvation*: Wiley: New York, 1985.

(68) Riddick, J. A.; Bunger, W. B.; Sakano, T. K. *Organic Solvents: Physical Properties and Methods of Purification*, 4th ed.; Wiley: New York, 1986.

(69) Fawcett, W. R.; Blum, L. *J. Chem. Soc., Faraday Trans* **1992**, *88*, 3339.

(70) Grampp, G.; Jaenicke, W. *Ber. Bunsen-Ges. Phys. Chem.* **1991**, *95*, 904.

(71) A value of $\Delta H^{\ddagger}_{L} = 0$ is assumed on the basis of the near temperature-independence of the second relaxation time of H_2O: Buchner, R.; Barthel, J.; Stauber, J. *Chem. Phys. Lett.* **1999**, *306*, 57.

(72) Blackbourn, R. L.; Hupp, J. T. *Inorg. Chem.* **1989**, *28*, 3786.

(73) Boeyens, J. C. A.; Forbes, A. G. S.; Hancock, R. D.; Wieghardt, K. *Inorg. Chem.* **1985**, *24*, 2926.

(74) Turner, J. W.; Schultz, F. A. *Inorg. Chem.* **1999**, *38*, 358.

(75) As no crystal structure of a $[Co(tacn)_2]^{3+}$ salt exists, the Co(III)-N distance is obtained from the crystal structure of $[Co((R)\text{-Metacn})_2]I_3 \cdot 5H_2O$, where Metacn is the 2-methyl derivative of 1,4,7-triazacyclononane: Mikami, M.; Kuroda, R.; Konno, M.; Saito, Y. *Acta Crystallogr.* **1977**, *B33*, 1485.

(76) Kuppers, H.-J.; Neves, A.; Pomp, C.; Ventur, D.; Wieghardt, K.; Nuber, B.; Weiss, J. *Inorg. Chem.* **1986**, *25*, 2400.

(77) Hupp, J. T.; Weaver, M. J. *J. Phys. Chem.* **1984**, *88*, 1463.

(78) Based on the thermodynamic parameters in ref 74, $[Fe(tacn)_2]^{2+}$ is 83% low-spin at the 295 K midpoint of the electrochemical rate measurements.[20]

(79) Wilson, R. B.; Solomon, E. I. *J. Am. Chem. Soc.* **1980**, *102*, 4085.

(80) König, E. *Struct. Bonding* **1991**, *76*, 51.

(81) Richardson, D. E.; Sharpe, P. *Inorg. Chem.* **1991**, *30*, 1412.